



1 Title

2

3 **Eddy Covariance Evaluation of Ecosystem Fluxes at a Temperate Saltmarsh in Victoria,**

4 **Australia Shows Large CO<sub>2</sub> Uptake**

5

6 Authors

7

8 Ruth Reef<sup>1</sup>,

9 Edoardo Daly<sup>2,3</sup>,

10 Tivanka Anandappa<sup>1</sup>,

11 Eboni-Jane Vienna-Hallam<sup>1</sup>,

12 Harriet Robertson<sup>1</sup>,

13 Matthew Peck<sup>1</sup>,

14 Adrien Guyot<sup>4,5</sup>

15

16 Affiliations

17

18 1 School of Earth, Atmosphere and Environment, Monash University, VIC 3800, Australia

19 2 Department of Civil Engineering, Monash University, VIC 3800, Australia

20 3 WMAwater, Brisbane, QLD 4000, Australia

21 4 Atmospheric Observations Research Group, The University of Queensland, Brisbane,

22 Australia

23 5 Australian Bureau of Meteorology, Melbourne, Australia

24

25 Corresponding Author

26

27 Associate Professor Ruth Reef

28 School of Earth Atmosphere and Environment

29 Monash University

30 9 Rainforest Walk, Clayton VIC 3800

31 Australia

32 Email: [ruth.reef@monash.edu](mailto:ruth.reef@monash.edu)



33 Ph: +61 3 9905 8309

34

35

36 Key Points

37

38 This is the first study using eddy covariance to measure CO<sub>2</sub> fluxes at an Australian  
39 temperate saltmarsh, revealing temperature and light limitations to CO<sub>2</sub> uptake.

40

41 CO<sub>2</sub> fluxes varied seasonally; growing season net ecosystem productivity was 10.54 g CO<sub>2</sub> m<sup>-2</sup>  
42 day<sup>-1</sup>, dropping to 1.64 g CO<sub>2</sub> m<sup>-2</sup> day<sup>-1</sup> in winter.

43

44 Annual productivity at the French Island saltmarsh is estimated at 753 g C m<sup>-2</sup> y<sup>-1</sup>, surpassing  
45 global saltmarsh estimates but below global mangrove averages.

46

47

48

49 Abstract

50

51 Recent studies highlight the important role of vegetated coastal ecosystems in atmospheric  
52 carbon sequestration. Saltmarshes constitute 30% of these ecosystems globally and are the  
53 primary intertidal vegetation outside the tropics. Eddy covariance (EC) is the main method  
54 for measuring biosphere-atmosphere fluxes, but its use in coastal environments is rare. At  
55 an Australian temperate saltmarsh site on French Island, Victoria, we measured CO<sub>2</sub> and  
56 water gas concentration gradients, temperature, wind speed and radiation. The marsh was  
57 dominated by a dense cover of *Sarcocornia quinqueflora*. Fluxes were seasonal, with minima  
58 in winter when vegetation is dormant. Net ecosystem productivity (NEP) during the growing  
59 season averaged 10.54 g CO<sub>2</sub> m<sup>-2</sup> day<sup>-1</sup> decreasing to 1.64 g CO<sub>2</sub> m<sup>-2</sup> day<sup>-1</sup> in the dormant  
60 period, yet the marsh remained a CO<sub>2</sub> sink due to some sempervirent species. Ecosystem  
61 respiration rates were lower during the dormant period compared with the growing season  
62 (1.00 vs 1.77 μmol CO<sub>2</sub> m<sup>-2</sup> s<sup>-1</sup>) with a slight positive relationship with temperature. During  
63 the growing season, fluxes were significantly influenced by light levels, ambient  
64 temperatures and humidity. Evapotranspiration peaked at 0.27 mm h<sup>-1</sup>. We cautiously



65 estimate the annual NEP budget at this marsh to be 753 ( $\pm 112.7$ ) g C m<sup>-2</sup> y<sup>-1</sup> which is similar  
66 to carbon uptake by temperate saltmarshes in Europe and within the range measured at  
67 some US saltmarshes. This value is higher than the value hypothesised for global  
68 saltmarshes of 382 g C m<sup>-2</sup> y<sup>-1</sup> but is only half the mean value estimated for global  
69 mangroves.

70

71 EGUsphere Topics

72 Emissions, Marine and Freshwater Biogeosciences, Earth System Biogeosciences

73

74 Short Summary

75

76 Studies show that saltmarshes excel at capturing carbon from the atmosphere. In this study,  
77 we measured CO<sub>2</sub> flux in an Australian temperate saltmarsh on French Island. The  
78 temperate saltmarsh exhibited strong seasonality. During the warmer growing season, the  
79 saltmarsh absorbed on average 10.5 grams of CO<sub>2</sub> from the atmosphere per m<sup>2</sup> daily. Even  
80 in winter, when plants were dormant, it continued to be a CO<sub>2</sub> sink, albeit smaller. Cool  
81 temperatures and high cloud cover inhibit carbon sequestration.

82

83

84

85



86 1. Introduction

87

88 Despite their relatively small global footprint of 54,650 km<sup>2</sup> (Mcowen et al., 2017), salt  
89 marshes provide a range of ecosystem services, including shoreline protection (Shepard et  
90 al., 2011), nutrient uptake, nursery grounds for fish populations (Whitfield, 2017) as well as  
91 functioning as significant carbon sinks through CO<sub>2</sub> uptake and storage in their organic rich  
92 sediments (McLeod et al., 2011). These ‘blue carbon’ habitats are recognised for their  
93 significant contribution to the global carbon cycle, as coastal wetlands more broadly are  
94 estimated to have accumulated more than a quarter of global organic soil carbon (Duarte,  
95 2017).

96

97 Saltmarshes are a widely distributed intertidal habitat but are floristically divergent globally  
98 (Adam, 2002), such that commonalities in function and form do not extend across  
99 biogeographic realms. US saltmarshes, for example, are extensively dominated by a single  
100 grassy species, *Spartina alterniflora*, as opposed to the dominance of C<sub>3</sub> Chenopodioideae  
101 species in the southern hemisphere (Adam, 2002). Temperate saltmarshes occupy a  
102 latitudinal range spanning from approximately 30° to 60° (Mcowen et al., 2017) and are  
103 most commonly found along protected coastlines such as bays, estuaries, and lagoons,  
104 where they are sheltered from the full force of wave action (Mitsch and Gosselink, 2000). In  
105 the Southern Hemisphere, temperate saltmarshes have a strong Gondwanan element with  
106 high floristic similarity among the marshes of New Zealand, the southernmost coasts of  
107 South America and South Africa and the southern coastlines of Australia (Adam, 1990).  
108 These marshes are often associated with extensive seagrass meadows and mudflats, and in  
109 parts of their range, mangroves, forming complex coastal mosaics (Huxham et al., 2018).  
110 Saltmarshes have been heavily degraded across their range, and it is estimated that perhaps  
111 up to 50% of the global saltmarsh area has been lost since 1900 (Gedan et al., 2009),  
112 primarily due to land use change.

113

114 Seasonality plays a major role in the functioning of temperate saltmarshes (Ghosh and  
115 Mishra, 2017). These ecosystems experience distinct growing and dormant seasons,  
116 primarily driven by temperature, light availability, and precipitation patterns (Adam, 2000).  
117 During the growing season (typically spring and summer), increased temperatures and



118 longer daylight hours stimulate plant growth, photosynthetic activity, and decomposition  
119 processes. Photosynthesis typically outpaces decomposition during this period, resulting in  
120 the temperate saltmarsh acting as a net CO<sub>2</sub> sink (Chmura et al., 2003). Conversely, the  
121 dormant season (usually fall and winter) is characterized by cooler temperatures and  
122 shorter days (Adam, 2000; Howe et al., 2010). These factors lead to reduced plant growth  
123 and photosynthetic activity (Adam, 2000) and while decomposition processes also slow  
124 down due to cooler temperatures, CO<sub>2</sub> release through decomposition often exceeds CO<sub>2</sub>  
125 uptake during this period (Artigas et al., 2015).

126

127 Gross primary production (GPP) of saltmarshes is the total photosynthetic flux of CO<sub>2</sub> from  
128 the atmosphere to the land surface, while respiration (R<sub>e</sub>) leads to a CO<sub>2</sub> flux directed back  
129 to the atmosphere. The difference between these two fluxes is the net ecosystem exchange  
130 (NEE). Saltmarsh ecosystems can act as both sources and sinks of carbon dioxide (CO<sub>2</sub>),  
131 influencing atmospheric CO<sub>2</sub> concentrations (Chmura et al., 2003). However, quantifying  
132 their net exchange remains challenging (Lu et al., 2017) hindering their effective inclusion in  
133 Earth System Models (Ward et al., 2020) and confounding the incorporation of saltmarsh  
134 restoration in emission reduction targets. Eddy covariance (EC) provides a powerful method  
135 for near-continuous, high-frequency monitoring of gas exchange between a vegetated  
136 surface and the atmosphere (Baldocchi, 2003), enabling the determination of net ecosystem  
137 exchange (NEE) of CO<sub>2</sub>, and identifying the forcings that determine how CO<sub>2</sub> fluxes will  
138 respond to global climate change (Borges et al., 2006; Cai, 2011).

139

140 Previous EC studies in coastal saltmarshes are limited to the Northern Hemisphere, in sites  
141 in the USA (e.g. Hill and Vargas, 2022; Kathilankal et al., 2008; Moffett et al., 2010; Nahrawi  
142 et al., 2020; Schäfer et al., 2019), France (Mayen et al., 2024), Japan (Otani and Endo, 2019)  
143 and China (Wei et al., 2020). The NEE values from these studies indicate that there is high  
144 inter-site (as well as interannual, Erickson et al., (2013)) variability in carbon dynamics of  
145 saltmarshes, with a link to species types, salinity, hydrology (Moffett et al., 2010; Nahrawi et  
146 al., 2020), site specific biochemical conditions (Seyfferth et al., 2020) and latitude (Feagin et  
147 al., 2020). While generally considered important carbon sinks (e.g. ranging between 130 to  
148 775 g C m<sup>-2</sup> yr<sup>-1</sup> in the USA, according to Kathilankal et al. (2008) and Wang et al.(2016)  
149 respectively) and globally hypothesised to average 382 g C m<sup>-2</sup> yr<sup>-1</sup> (Alongi, 2020), some EC



150 studies revealed saltmarshes to be net sources of CO<sub>2</sub> to the atmosphere (Vázquez-Lule and  
151 Vargas, 2021) especially in temperate saltmarshes that experience long dormant periods.

152

153 The aim of this study is to estimate CO<sub>2</sub> and water fluxes in a temperate saltmarsh in  
154 Victoria, southern Australia, to better characterise the effect of seasonality and  
155 environmental variables on the saltmarsh CO<sub>2</sub> budgets. This is the first study in an Australian  
156 coastal saltmarsh where CO<sub>2</sub> fluxes are estimated using the EC method.

157

158 2. Methods

159

160 2.1 Site Description

161

162 Ecosystem flux measurements were collected at the Tortoise Head Ramsar coastal wetland  
163 on French Island, Victoria (38.388°S, 145.278°E, Fig. 1) within the Western Port embayment.

164 French Island is within the Cfb climate zone (temperate oceanic climate) and experiences

165 distinct seasonal variations in temperature and precipitation. Long term (30 year) climate

166 data averaged from the nearby Cerberus Station (Australian Bureau of Meteorology, site

167 86361) indicated that summers, spanning from December through February, are generally

168 mild to warm, with maximum temperatures typically ranging from 17°C to 25°C although

169 occasional heatwaves lead to temporary spikes in temperature that can exceed 30°C.

170 Winters, from June to September, are cooler, with maximum temperatures ranging

171 between 7°C and 14°C and a mean minimum temperature of 6°C. Frost is infrequent due to

172 maritime influence, though crisp mornings below 0°C occur 10% of the time in winter.

173 Rainfall, evenly distributed throughout the year, averages ca. 715 mm y<sup>-1</sup>, although in 2020

174 the site experienced higher than average rainfall (860 mm y<sup>-1</sup>). The island is exposed to

175 weather patterns influenced by the Southern Ocean and Bass Strait, leading to occasional

176 storm systems, particularly in winter, bringing gusty winds and increased precipitation.

177 Western Port has semi-diurnal tides with a range of nearly 3 m, resulting in wide intertidal

178 flats occupied by mangroves of the species *Avicennia marina* and saltmarshes.

179



180

181

182 Figure 1: a) The location of French Island along the Bass Strait coast of Australia, and b) The  
183 location of the flux tower on French Island as well as the nearby Cerberus meteorological  
184 station (Bureau of Meteorology, Australia), © Google Earth. c) An image of the saltmarsh  
185 within the flux tower footprint during the growing season (with the tower and the author in  
186 the background), taken in February 2020 by Prudence Perry. d) an image of the saltmarsh  
187 during the dormant period, taken at the same location in September 2020 by Ruth Reef.

188

189 The site at French Island is dominated by an extensive temperate coastal saltmarsh  
190 community that is a particularly good natural representation of a broader biogeographic  
191 saltmarsh grouping which covers an area of ca. 7000 ha along Victoria's central coast  
192 embayments (Navarro et al., 2021). While the wetland at the site is a saltmarsh-mangrove-  
193 seagrass wetland system, the footprint of the flux tower was limited to the saltmarsh alone,  
194 which extends more than a kilometre from the shoreline in places. This geography provided  
195 the critical horizontally homogenous area with flat terrain required for ecosystem flux  
196 measurements. Floristically this saltmarsh is species poor, dominated by *Sarcocornia*



197 *quinqueflora*. Stands of *Tecticornia arbuscula* are common in this saltmarsh, while *Atriplex*  
198 *cinerea*, *Suaeda australia* and *Distichis distichophylla* can be prevalent depending on  
199 elevation and soil drainage conditions. *Sarcocornia quinqueflora* is a perennial succulent and  
200 at the temperate ranges of its distribution it has a distinct growing season from October to  
201 May (Fig. 1c) when the stems turn red, followed by a woody and fibrous dormant period  
202 during the colder months of June through September (Fig. 1d). The height of the dominant  
203 vegetation ranged between 0.3-0.6 m.

204

## 205 2.2 Data Collection and Analysis

206

207 Eddy covariance measurements were made between November 2019 and August 2021  
208 capturing both the saltmarsh growing season (October-March) as well as a dormant period  
209 (April-September). An array of standard micro-meteorological instruments included a 3-  
210 dimensional sonic anemometer (CSAT3, Campbell Scientific, USA), an open-path infra-red  
211 carbon dioxide (CO<sub>2</sub>) gas and water vapour (H<sub>2</sub>O) analyser (Li-7500, Li-Cor, USA) and 2 data-  
212 loggers. The tower was powered by a solar array with two accompanying 12V DC storage  
213 batteries. The sonic anemometer was mounted 2.3 m above ground. The CO<sub>2</sub>/H<sub>2</sub>O gas  
214 analyser was mounted 0.11 m longitudinally displaced from the anemometer. A CR3000  
215 datalogger (Campbell Scientific, USA), recorded the Li-7500, anemometer, short- and long-  
216 wave radiation (CNR4, Klip & Zonen, the Netherlands), air temperature and humidity (083E,  
217 Met One, USA) readings at 10 Hz frequency. Due to the location of the site in the Bass Strait  
218 (a region that experiences regular winter storms, high wind speeds and higher than national  
219 average cloud cover) the tower sustained damage due to winter storms several times during  
220 the deployment, as well as suffered periods of poor power supply due to short day lengths  
221 and high cloud cover; this was exacerbated by poor accessibility to the remote location  
222 during COVID-19 travel restrictions. The analysis, thus focused on extended periods of  
223 continuous daily records and periods with large gaps in the dataset were removed.

224

225 Ecosystem fluxes were calculated for 30 min intervals using Eddy Pro software v.7 (LI-COR  
226 Inc., USA) Express Mode protocols. This processing step includes coordinate axis rotation  
227 correction, trend correction, data synchronisation, statistical tests for quality, density  
228 corrections and spectrum corrections. As part of this step, flux quality flags were assigned to





229 the calculated CO<sub>2</sub> fluxes using the 0–2 flag policy ‘Mauder and Foken 2004’, based on the  
230 steady state test and the developed turbulent conditions test. Only data that met the  
231 criteria of being in quality class 0 (‘best quality fluxes’) for CO<sub>2</sub> flux were chosen for further  
232 analysis. We further removed anomalous data points defined as values that exceeded four  
233 standard deviations from the mean CO<sub>2</sub> flux; this resulted in the additional loss of ca. 1% of  
234 the dataset. Gap filling was not applied. Additional filtering was applied to night-time data  
235 due to known weak convection at night, thus CO<sub>2</sub> flux data during periods of atmospheric  
236 stability, i.e. when night friction wind velocities ( $u^*$ ) were below 0.2 m s<sup>-1</sup>, were excluded.  
237 This resulted in a dataset of 674 day-time and 606 night-time flux measurements during the  
238 dormant period and 4124 day-time and 3020 night-time flux measurements for the growing  
239 period. The growing season dataset included 90 days with 85% or more flux data coverage,  
240 while the dormant season dataset included 18 days and these days were used for 24-hour  
241 flux integrations.

242

243 Half-hourly average CO<sub>2</sub> flux was measured in  $\mu\text{mol m}^{-2} \text{s}^{-1}$ , with positive fluxes indicating a  
244 flux direction from the Earth’s surface to the atmosphere. Net ecosystem exchange (NEE)  
245 was defined as the net flux of CO<sub>2</sub> from the atmosphere to the marsh and was often  
246 negative during daytime, indicating that Gross Primary Productivity (GPP) was larger than  
247 ecosystem respiration ( $R_e$ ). Evapotranspiration (ET) was calculated by Eddy Pro as the ratio  
248 between the latent heat flux (LE) and latent heat of vaporisation ( $\lambda$ ). Ecosystem water use  
249 efficiency (WUE<sub>e</sub>) was then expressed as the ratio between daytime net ecosystem  
250 productivity in  $\text{g CO}_2 \text{ m}^{-2} \text{ h}^{-1}$  and evapotranspiration in  $\text{mm h}^{-1}$ .

251

252 A two-dimensional footprint estimation was provided according to the simple footprint  
253 parameterisation described in Kljun et al. (2015) calculating the ground position of the  
254 cumulative fraction of flux source contribution by distance for each 30-minute interval. We  
255 assessed the short-term effects of environmental factors on CO<sub>2</sub> fluxes at a half-hourly time  
256 scale (e.g. the effects of light, air temperature and vapour pressure deficit) using a series of  
257 non-linear or linear models. These analyses were limited to the growing season, when the  
258 plants were actively photosynthesising. The integrated CO<sub>2</sub> and H<sub>2</sub>O fluxes over time (i.e.,  
259 the daily sum of CO<sub>2</sub> or H<sub>2</sub>O flux) were calculated for days with complete records (data



260 density>80%) as the area under the curve for each 24-hour period according to the  
261 trapezoid rule. All post-processing and statistical analyses were performed in R 4.3.2.

262

263 Because of the large data gaps, it was not possible to model the partition of the NEE in GEP  
264 and  $R_e$  using common partitioning methods (Lasslop et al., 2010). For simplicity, it was  
265 assumed that NEE at night coincided with  $R_e$ .  $R_e$  was corrected for temperature effects on  
266 respiration using the linear slope of the relationship between night-time NEE and  
267 temperature. For the CO<sub>2</sub> budget, Net Ecosystem Production (NEP), defined as  $NEP = -NEE$ ,  
268 and Gross Ecosystem Production (GEP), defined as  $GEP = -GPP$ , were used.

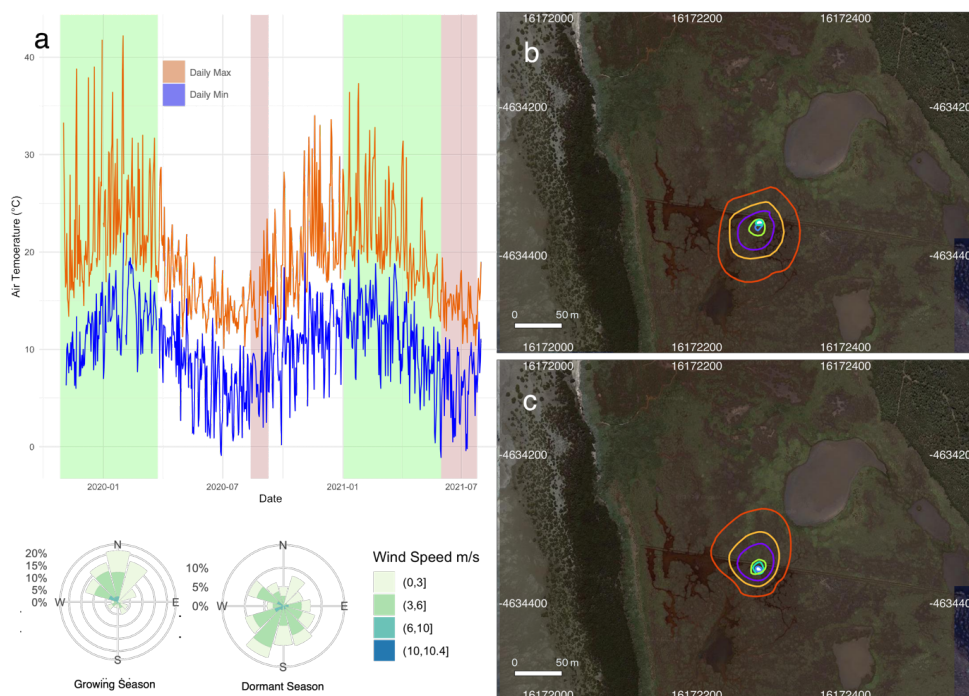
269

### 270 3. Results

271

272 The observations were divided into a growing season and a dormant season to reflect the  
273 seasonal phenology of the dominant vegetation type within the flux tower footprint, which  
274 has a relatively short growing season during the summer. During the growing season, mean  
275 temperature averaged 22.3°C. Several heatwaves occurred during this period, with  
276 temperatures exceeding 40°C on a few occasions in 2019. The dormant season was  
277 significantly colder and windier, with frequent southerly winds (Fig. 2a). Footprint models  
278 showed a slight variation in flux source between the two seasons, although in both cases the  
279 size of the footprint and the vegetation composition within the footprint was similar (Figs.  
280 2b and 2c), but the shape was skewed to the north during winter due to the prevalent  
281 southerly winds in that season (Fig. 2a). 70% of the flux measurement source was from  
282 within 50 m of the tower, while the maximum length of the source location was 73 m.

283



284

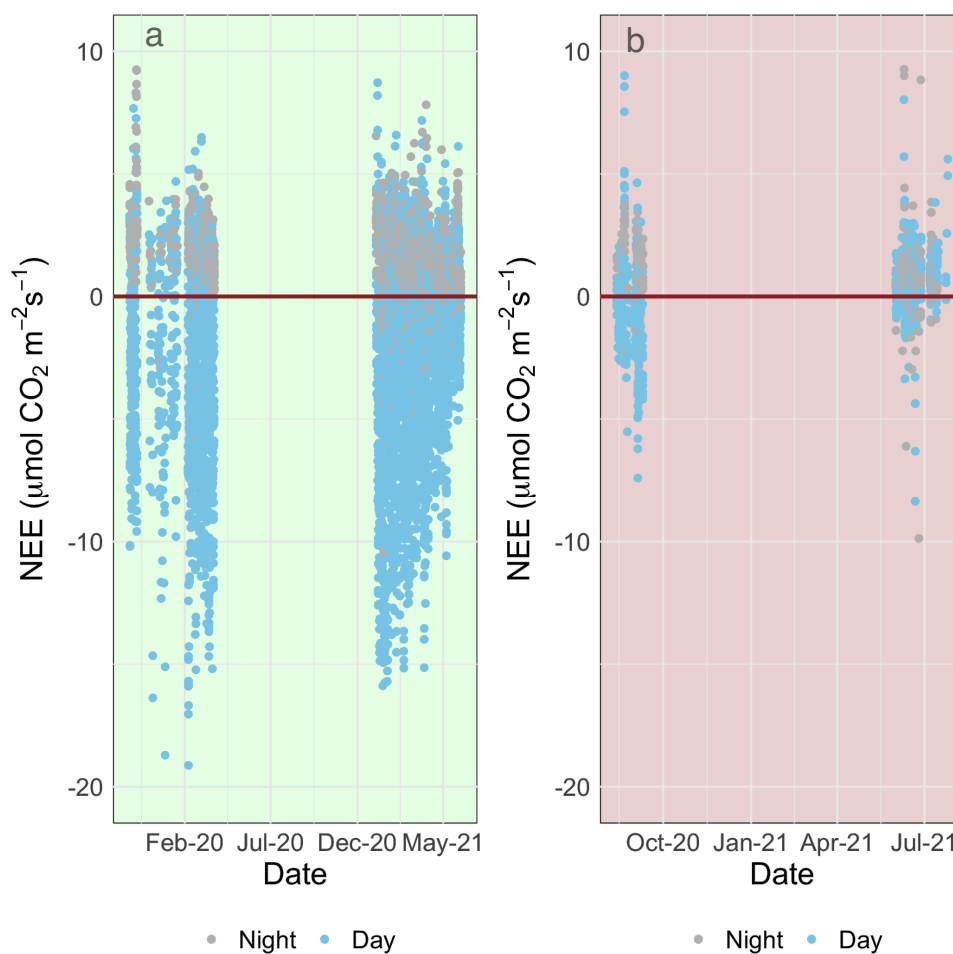
285

286 Figure 2: a) The minimum and maximum daily temperature recorded at the Cerberus  
 287 meteorological station (Bureau of Meteorology, Fig. 1b) during 2019-2021. The marsh  
 288 growing (Nov-Mar) and dormant (Aug-Sep) periods observed during this study are  
 289 highlighted. A corresponding wind rose diagram summarises the wind speeds and directions  
 290 measured at the tower site during the observation periods. The flux source footprint  
 291 surrounding the tower during the dormant season (b) and the growing season (c) shows the  
 292 cumulative flux source contribution to the flux measurements, with the outer red line  
 293 representing the distance by which 90% of the calculated flux is sourced and the other  
 294 isolines from the tower outwards correspond to 10%, 20%, 40%, 60% and 80% of the flux.  
 295

296 The growing season dataset included 90 days with 80% or more flux data coverage, while  
 297 the dormant season dataset included 18 days. There was a strong temporal variability in net  
 298 ecosystem exchange (NEE) across both short (daily) and long (seasonal) temporal scales (Fig.  
 299 3). Daytime fluxes were defined as flux points where the global radiation values in the flux  
 300 averaging half-hour interval were  $>12 \text{ W m}^{-2}$ . At the diurnal scale, saltmarsh NEE were



301 negative mostly during the day and positive mostly during the night and ranged between -  
302 19.1 and 10.86  $\mu\text{mol m}^{-2} \text{s}^{-1}$  across the measurement periods.  
303



304

305

306 Figure 3: A time series of half-hourly measurements of CO<sub>2</sub> flux between a temperate  
307 saltmarsh and the atmosphere measured by eddy covariance during the marsh growing  
308 season (a) and the dormant season (b). Blue and grey points indicate measurements taken  
309 during day-time and night-time respectively. Positive fluxes indicate a direction of flux from  
310 the Earth surface to the atmosphere.

311

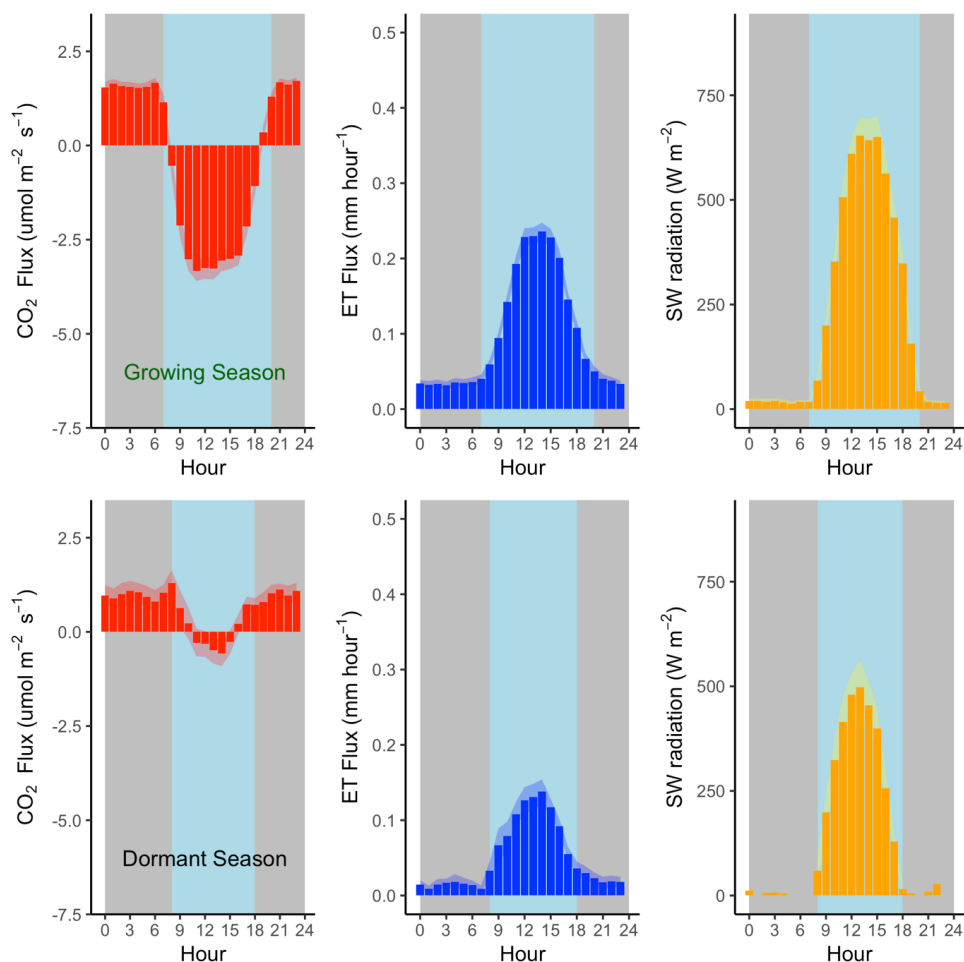


312 Flux rates varied across the day, with CO<sub>2</sub> uptake peaking at 11:00 during the growing  
313 season, and later in the day (14:00) during the dormant period (Fig. 4). Ecosystem  
314 respiration rates ( $R_e$ , defined as night-time CO<sub>2</sub> flux) were on average ( $\pm$ SD) 1.77 ( $\pm$ 1.12)  
315  $\mu\text{mol m}^{-2} \text{s}^{-1}$  during the growing season and 1.0 ( $\pm$  0.93)  $\mu\text{mol m}^{-2} \text{s}^{-1}$  during the dormant  
316 period. The difference in ecosystem respiration between the growing and dormant seasons  
317 is highly significant (t-test,  $p < 0.01$ ). Daytime CO<sub>2</sub> flux was on average ( $\pm$ SD) -3.53 ( $\pm$  4.15)  
318  $\mu\text{mol m}^{-2} \text{s}^{-1}$  during the growing season and -0.25 ( $\pm$  2.18)  $\mu\text{mol m}^{-2} \text{s}^{-1}$  during the dormant  
319 season. Thus, we derive that the maximum Gross Primary Productivity (GPP) of this  
320 ecosystem from NEE and temperature-corrected  $R_e$ , measured during the growing season,  
321 is ca.  $-5.34 \pm 4.3 \mu\text{mol CO}_2 \text{ m}^{-2} \text{ s}^{-1}$  ( $-5.53 \pm 4.45 \text{ g C m}^{-2} \text{ day}^{-1}$ ). Average  $R_e$  is thus estimated to  
322 comprise 33% of GPP.

323

324 Mean ( $\pm$ SD) daily evapotranspiration was 2.48 mm ( $\pm$ 2.79 mm) during the growing season  
325 and 0.97 mm ( $\pm$ 1.35 mm) during the dormant season (Fig. 4). Evapotranspiration peaked at  
326 noon AEST during the growing season (0.26 mm h<sup>-1</sup>), and later in the day (14:00 AEST)  
327 during the dormant season (0.14 mm h<sup>-1</sup>).

328



329

330

331 Figure 4: Mean hourly CO<sub>2</sub> and H<sub>2</sub>O flux (evapotranspiration) rates during the growing  
332 season (top) and the dormant season (bottom) alongside mean short wave incoming  
333 radiation. Shading corresponds to 1 standard deviation around the mean. Grey plot  
334 background approximates night-time periods, while light blue approximates daytime (actual  
335 day length varies within each season).

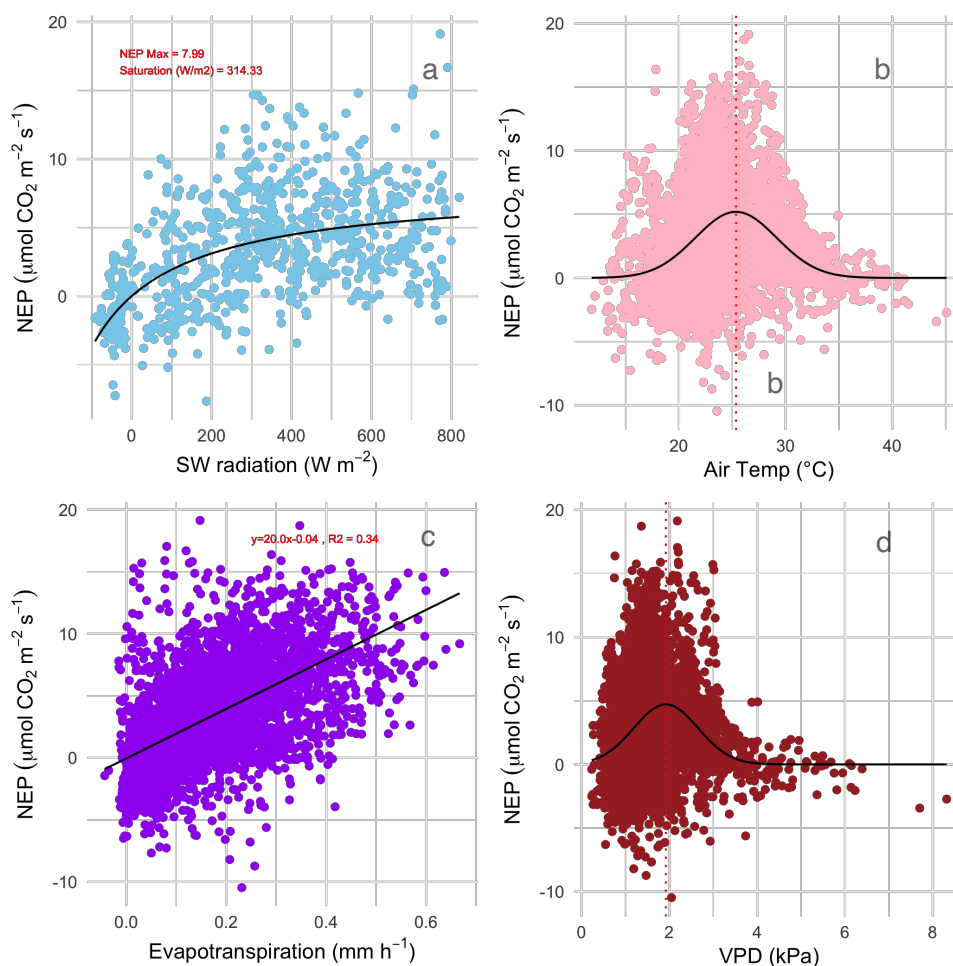
336

337 The effect of some environmental forcings on daytime NEE during the saltmarsh growing  
338 season were explored (Fig. 5). To distinguish this daytime-only value from the 24-hour  
339 carbon balance integration, and to better highlight CO<sub>2</sub> uptake, NEP values are shown.

340



341 Short wave radiation (visible light) was a limiting factor to NEP below approximately 300 W  
342  $\text{m}^{-2}$ , but radiation did not reach damaging levels that would lead to a drop in NEP  
343 throughout the measurement range, which reached a maximum level of ca. 800  $\text{W m}^{-2}$ .  
344 Unlike light, the NEP-air temperature relationship followed a Gaussian response, with the  
345 highest NEP achieved at the optimal temperature of 25.3°C with a standard deviation of  
346 3.8°C followed by a decline in  $\text{CO}_2$  uptake by the marsh at higher temperatures. The  
347 minimum and maximum air temperatures for which modelled NEP nears zero (defined here  
348 as 3 standard deviations from the mean) are 13.9°C and 36.7°C respectively. Temperature  
349 also had a slight but significant positive linear relationship with ecosystem respiration  
350 (slope=0.07  $\mu\text{mol CO}_2 \text{ m}^{-2} \text{ s}^{-1} \text{ }^\circ\text{C}^{-1}$ ,  $p < 0.01$ , data not shown).  
351  
352 NEP was positively correlated with evapotranspiration during the growing season (Pearson  $r$   
353 = 0.59, Fig.5 C). The slope of the NEP/ET relationship was 20.0, indicating an ecosystem  
354 water use efficiency ( $\text{WUE}_e$ ) of 0.86  $\text{g C kg}^{-1} \text{ H}_2\text{O}$  ( $R^2 = 0.34$ ,  $p < 0.001$ ). The response of NEP to  
355 atmospheric vapour pressure deficit (VPD) fit a Gaussian relationship (the commonly  
356 observed inverse U-shaped curve relationship in response to VPD in plants), with NEP  
357 declining rapidly when VPD exceeded 2.39 kPa. The optimal range of VPD within which NEP  
358 was maximised in this ecosystem was 1.92 kPa ( $\pm 0.73$  kPa).  
359



360

361 Figure 5: The relationship between growing season net ecosystem  $\text{CO}_2$  uptake (NEP,  $\mu\text{mol}$   
 362  $\text{CO}_2 \text{ m}^{-2} \text{ s}^{-1}$ ) and corresponding environmental variables. a) Shortwave radiation (visible  
 363 light); black line is the Michaelis-Menten model of best fit. The coefficient of saturation is at  
 364  $314 \text{ W m}^{-2}$  and maximum net productivity is  $8.0 \mu\text{mol CO}_2 \text{ m}^{-2} \text{ s}^{-1}$ . b) Air temperature; black  
 365 line is a Gaussian model of best fit with a temperature optimum at  $25.3^{\circ}\text{C}$ . c)  
 366 Evapotranspiration; linear model ( $R^2 = 0.34$ ) has a slope of  $20.0$ . d) Vapour Pressure Deficit;  
 367 black line is a Gaussian model of best fit with a VPD optimum at  $1.92 \text{ kPa}$ .

368

369 When integrated over a 24-hour period, the saltmarsh is on average a  $\text{CO}_2$  sink during all  
 370 canopy phenological phases (Fig. 6), although during the dormant season the sink is weaker,  
 371 with an average uptake of  $-2.42 \text{ g CO}_2 \text{ m}^{-2} \text{ day}^{-1} (\pm 2.54)$ . During the growing season (defined

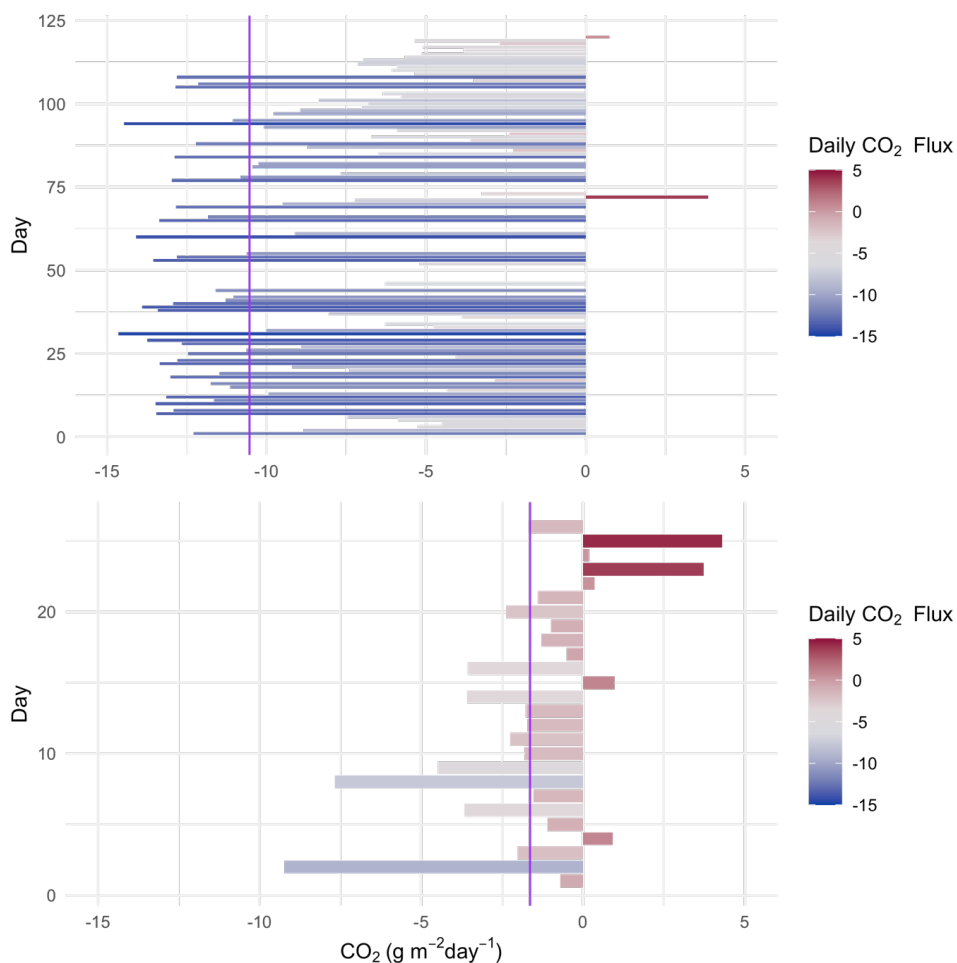




372 as the non-dormant period and thus reflecting several phenological stages), the marsh is a  
373 substantial sink with a mean ( $\pm$ SD) daily NEP of  $10.95 \text{ g CO}_2 \text{ m}^{-2} \text{ day}^{-1}$  ( $\pm 4.98$ ) over a 24-hour  
374 period (ranging between  $-22.8$  and  $4.3 \text{ g of CO}_2 \text{ emission to the atmosphere m}^{-2} \text{ day}^{-1}$ ). The  
375 daily  $\text{CO}_2$  budget during the growing season showed some variability among days ( $\text{CV}=0.46$ ,  
376 Fig. 6) and days with lower average light levels (i.e. cloudy days) had a significant negative  
377 impact on the  $\text{CO}_2$  budget (multiple linear regression,  $p < 0.02$ ,  $R^2 = 0.27$ ). Daily maximum air  
378 temperatures did not have a significant impact on the daily  $\text{CO}_2$  budget ( $p = 0.77$ ) at this  
379 location, although NEE was significantly affected by temperature at finer temporal scales  
380 (Figure 5). Assuming the dormant period spans a third of the year, we cautiously estimate  
381 an annual NEP value of  $753 (\pm 112.7) \text{ g C m}^{-2} \text{ yr}^{-1}$ .

382

383



384

385

386 Figure 6: Daily (24 h) integrated NEE in  $\text{g CO}_2 \text{ m}^{-2} \text{ day}^{-1}$  during the saltmarsh growing season

387 (top) and the dormant season (bottom) for days with data density > 85%. Purple lines

388 indicate the mean daily integrated flux for each season ( $-10.54$  and  $-1.64 \text{ g CO}_2 \text{ m}^{-2} \text{ day}^{-1}$

389 with an SD of  $4.98$  and  $2.54$  for growing and dormant respectively). A positive balance

390 indicates an integrated net flux of  $\text{CO}_2$  from the Earth's surface to the atmosphere over the

391 24-hour period. Assuming the dormant season period spans one third of the year, we

392 cautiously estimate an annual NEP value of  $753 \text{ g C m}^{-2} \text{ yr}^{-1}$  ( $\pm$ weighted sum of SD of  $5.9$ ).

393

394

395 4. Discussion



396

397 At this temperate saltmarsh, seasonality had a significant effect on carbon and water flux.  
398 Growing season net ecosystem productivity was five times greater than during the dormant  
399 period. Seasonality in Australian marshes has not been previously reported in the scientific  
400 literature, and assumptions were made that Australian saltmarshes do not exhibit the  
401 growing and dormant phenology observed on other continents (Clarke and Jacoby, 1994).  
402 Seasonality might be an overlooked important characteristic of this habitat and in addition  
403 to affecting flux estimations, can have broader implications. For example, in the USA, the  
404 saltmarsh greening up period was shown to be an important range-wide timing event for  
405 migratory birds (Smith et al., 2020) with plant-growth metrics predicting the timing of nest  
406 initiation for shorebirds. Saltmarshes in Australia are important roosting and feeding sites  
407 along the East Asian Australasian Flyway, particularly waders, thus potentially a similar  
408 relationship between migration timing and saltmarsh phenology could be occurring.  
409 Seasonality also affects other significant ecosystem functions such as the bio-  
410 geomorphological feedback between saltmarshes, coastal hydrodynamics and landscape  
411 evolution (Reents et al., 2022).

412

413 We derived the light-response and associated coefficients of light regulation of saltmarsh  
414 NEE using the Michaelis-Menten model (Chen et al., 2002). Quantum (or production)  
415 efficiency is the predominant input in remote sensing techniques to model productivity, and  
416 is specific to the biome (Hilker et al., 2010). While not directly comparable to leaf level  
417 quantum efficiency measurements, the quantum efficiency ( $\alpha$ ) of the NEP light response  
418 curve was estimated from the slope of the Michaelis-Menten model to be  $0.025 \mu\text{mol CO}_2 \text{ J}^{-1}$ .  
419 The ecosystem reached light saturation at an insolation of  $314 \text{ W m}^{-2}$ , but daytime  
420 insolation was below this value more than 50% of the time suggesting that light might be a  
421 significant limiting factor to NEP at this marsh, especially during winter. The level of light  
422 limitation we observed is an underestimation, due to the loss of high-quality EC data during  
423 periods of rain. The solar geometry at this latitude and the length of day result in an annual  
424 average top of atmosphere SW radiation of  $250 \text{ W m}^{-2}$ , but clouds can strongly modulate  
425 the SW radiation balance (SWCRE), and apart from the months of January and February  
426 when cloudy days are less frequent (10-12 days per month), cloudy days are frequent at this



427 site, averaging 15-17 days per month (Bureau of Meteorology) and could significantly  
428 impact on NEP.

429

430 Temperature is another forcing that significantly impacts NEE at this marsh, with an optimal  
431 range for maximum NEP at 25.3°C (21.5°C-29.1°C). Data for Australian saltmarshes is not  
432 available, but this optimal temperature response range is similar to that measured  
433 experimentally in a saltmarsh species in an equivalent climate zone (e.g. Georgia,  
434 (Giurgevich and Dunn, 1981)) and to the values hypothesised for the habitat from data  
435 collected along the US Atlantic Coast, (Feher et al., 2017). The long-term average maximum  
436 daytime temperature at this site is 19.2°C, which is cooler than the optimal range for NEE  
437 suggesting temperature can be a significant limiting factor to productivity, especially during  
438 the dormancy period where average monthly maximum temperatures are only 13.7°C to  
439 16.6°C (Bureau of Meteorology). During the growing season the average maximum  
440 temperatures are within the range of optimal NEE (20.6°C to 23.1°C), although hot days  
441 (>30°C) significantly depress NEE and depending on the year, can be common during  
442 summer months (averaging 2-6 days per month).

443

444 In saltmarshes, evapotranspiration occurs from plant mediated transpiration but also from  
445 soil pores (which tend to be saturated), wetted leaves and open water. We observed  
446 average evaporation rates of 2.48 mm day<sup>-1</sup> during the growing season and 0.97 mm day<sup>-1</sup>  
447 during the dormant season. Actual evapotranspiration in this region modelled using the  
448 CMRSET algorithm is estimated to range between 0.6 and 3.2 mm day<sup>-1</sup> during winter and  
449 summer respectively (McVicar et al., 2022); these values are consistent with our field  
450 measurements. Overall, rainfall is in excess of the requirements for maintaining ET at this  
451 site, although deficits can develop for short periods during the growing season.

452 Long term rainfall excess could be contributing to the complicated hydrology at this  
453 location, where inundation is not strictly associated with tidal stage (data not shown).

454 Growing season ET rates are significantly higher than those of the dormant season, partly  
455 due to the solar configuration in winter as opposed to summer, but also due to phenological  
456 changes. A big leaf model estimation of evapotranspiration from saltmarshes in New South  
457 Wales estimates ET to be highly sensitive to vegetation height, increasing by more than 1  
458 mm day<sup>-1</sup> as vegetation height increases from 0.1 to 0.4 m (Hughes et al., 2001) and



459 transpiration in saltmarsh plants in the cold season has been shown to account for only 20%  
460 of the annual transpiration budget (Giurgevich and Dunn, 1981) following the same pattern  
461 as the seasonal distribution of productivity.

462

463 The rate of carbon uptake per unit of water loss (WUE) is a key ecosystem characteristic,  
464 which is a result of a suite of physical and canopy physiological forcings, and has direct  
465 implications for ecosystem function and global water and carbon cycling. Mean water use  
466 efficiency (WUEe) of this saltmarsh was estimated at  $0.86 \text{ g C kg}^{-1} \text{ H}_2\text{O}$ , which is markedly  
467 lower than for grass dominated saltmarshes in China ( $2.9 \text{ g C kg}^{-1} \text{ H}_2\text{O}$ , Xiao et al. (2013)) but  
468 similar to the value for WUEe based on NEP and ET in mangroves ( $0.77 \text{ g C kg}^{-1} \text{ H}_2\text{O}$ , Krauss  
469 et al. (2022)). The chenopod *Sarcocornia quinqueflora* has been suspected to have higher  
470 evapotranspiration rates than saltmarsh grasses by approx. 15% (Hughes et al., 2001), but  
471 while *Sarcocornia quinqueflora* dominates at this site, the footprint is a mix of species and  
472 the lower WUEe cannot be directly linked to the presence of *Sarcocornia quinqueflora*.

473 Furthermore, like most wetlands, the wetland surface is a mixed composition of emergent  
474 vegetation, unsaturated soil and water bodies thus the spatial scale at which WUEe is  
475 determined encompasses both the canopy ( $E_c$ ) as well as any open water present in the  
476 footprint. Transpiration is predicted to account for only 55% of ET in these systems (Hughes  
477 et al., 2001), which is an  $E_c$  to ET ratio similar to that of mangroves (Krauss et al., 2022) but  
478 significantly lower than terrestrial forests where more than 90% of ET can be attributed to  
479 transpiration. Thus, regional variations in WUEe can be attributed to multiple forcings that  
480 form complex spatiotemporal patterns.

481

482 Saltmarshes are considered among the most productive ecosystems on Earth with an  
483 estimated global NEP of  $634 \text{ Tg C y}^{-1}$  (Fagherazzi et al., 2013). Productivity of southern  
484 Australian marshes was previously estimated at  $0.8 \text{ kg m}^{-2} \text{ y}^{-1}$  by repeated measurements of  
485 above ground standing crops (Clarke and Jacoby, 1994), which is remarkably similar to the  
486 values reported here, where we extrapolate an approximate annual mean of  $0.75 \text{ kg C m}^{-2} \text{ y}^{-1}$ .  
487 Similar studies on saltmarshes in France report lower productivity than the marshes at  
488 French Island ( $-483 \text{ g C m}^{-2} \text{ y}^{-1}$ , (Mayen et al., 2024)) but our values are within the range  
489 reported for mid-latitude saltmarsh sites in the USA ( $-775 \text{ g C m}^{-2} \text{ y}^{-1}$ , (Wang et al., 2016))  
490 and China ( $-668 \text{ g C m}^{-2} \text{ y}^{-1}$ , (Xiao et al., 2013)). It is clear that productivity across climate



491 zones and biogeographic regions varies widely with some studies even reporting net  
492 emissions over an annual period from some marshes and a global average estimated  
493 between -382 (Alongi, 2020) and -1,585 g C m<sup>-2</sup> y<sup>-1</sup> (Chmura et al., 2003), albeit based on a  
494 small subset of studies. An analysis of GPP across latitudes in the USA show that warmer  
495 sites (including mangrove wetlands in southern USA) had significantly higher GPP than mid-  
496 latitude saltmarshes such as the one on French Island (Feagin et al., 2020). Mangroves have  
497 higher NEE than saltmarshes, estimated by (Krauss et al., 2022) to average 1200 g C m<sup>-2</sup> y<sup>-1</sup>.  
498 The data presented here is the exchange of carbon between the land surface and the  
499 atmosphere, but saltmarshes, like other marine connected communities, exchange carbon  
500 also through dissolved carbon pathways, which can be significant (Cai, 2011). Thus, the  
501 fluxes presented here do not constitute the entire carbon budget of this ecosystem.

502

## 503 5. Conclusions

504

505 The response of the French Island saltmarsh to environmental drivers is indicative of the  
506 complex interactions determining saltmarsh productivity. While the overall carbon  
507 sequestration rate we measured was in the range of other temperate saltmarsh estimates  
508 (ca. 750 g C m<sup>-2</sup> y<sup>-1</sup>), the unique long-term, high-resolution record enabled us to derive  
509 temperature, VPD and light response functions, thus formulating equations that describe  
510 how climate-change sensitive parameters such as temperature, relative humidity, and cloud  
511 cover, affect CO<sub>2</sub> uptake, respiration and evapotranspiration. The marsh operated as a CO<sub>2</sub>  
512 sink throughout the various canopy phenological phases, but during the dormant period,  
513 CO<sub>2</sub> uptake was less than 25% that of the growing season. Seasonality has not been  
514 previously considered in Australian saltmarshes and it should not be overlooked when  
515 estimating saltmarsh carbon budgets.

516

## 517 Competing interests

518

519 The contact author has declared that none of the authors has any competing interests.

520

## 521 Acknowledgments

522



523 The work was carried out with the permission of Parks Victoria (Permit 10008684). We thank  
524 Phil and Yuko Bock for logistic support and accommodation on French Island. We thank  
525 Leigh Burgess, Kiri Mason and Ian McHugh for technical support and the Australian OzFlux  
526 community for ongoing collaboration. This work was funded by an Australian Research  
527 Council Discovery Award to RR and ED (DP220102873) as well as a Monash University  
528 Networks of Excellence award to RR.

529

#### 530 Data Availability

531 Data used for this analysis is available at <https://figshare.com/s/ba62aafd1a4049248a08>  
532 (note that this is a temporary private link to an embargoed dataset which will be replaced  
533 with a publicly available DOI upon publication).

534

#### 535 Author contribution

536 RR conceptualised the study, acquired funding, prepared the manuscript, designed and  
537 carried out the field campaign, and performed the analysis. ED acquired funding, developed  
538 methodology and prepared the manuscript. AG developed methodology and prepared the  
539 manuscript. TA, EJVH, HR and MP were involved in the field investigation and administration  
540 of the project and provided edits on the manuscript.

541

#### 542 References

543

544 Adam, P.: Saltmarsh Ecology, Cambridge University Press, 1990.

545 Adam, P.: Morecambe Bay saltmarshes: 25 years of change, in: British Saltmarshes, Forrest  
546 Text, Cardigan, UK, 81–107, 2000.

547 Adam, P.: Saltmarshes in a time of change, *Environ. Conserv.*, 29, 39–61,  
548 <https://doi.org/10.1017/S0376892902000048>, 2002.

549 Alongi, D. M.: Carbon balance in salt marsh and mangrove ecosystems: A global synthesis, *J.*  
550 *Mar. Sci. Eng.*, 8, 767, 2020.

551 Artigas, F., Shin, J. Y., Hobbie, C., Marti-Donati, A., Schäfer, K. V. R., and Pechmann, I.:  
552 Long term carbon storage potential and CO<sub>2</sub> sink strength of a restored salt marsh in New  
553 Jersey, *Agric. For. Meteorol.*, 200, 313–321, <https://doi.org/10.1016/j.agrformet.2014.09.012>,  
554 2015.



- 555 Baldocchi, D. D.: Assessing the eddy covariance technique for evaluating carbon dioxide  
556 exchange rates of ecosystems: past, present and future, *Glob. Change Biol.*, 9, 479–492,  
557 <https://doi.org/10.1046/j.1365-2486.2003.00629.x>, 2003.
- 558 Borges, A. V., Schiettecatte, L.-S., Abril, G., Delille, B., and Gazeau, F.: Carbon dioxide in  
559 European coastal waters, *Trace Gases Eur. Coast. Zone*, 70, 375–387,  
560 <https://doi.org/10.1016/j.ecss.2006.05.046>, 2006.
- 561 Cai, W.-J.: Estuarine and coastal ocean carbon paradox: CO<sub>2</sub> sinks or sites of terrestrial  
562 carbon incineration?, *Annu. Rev. Mar. Sci.*, 3, 123–145, [https://doi.org/10.1146/annurev-](https://doi.org/10.1146/annurev-marine-120709-142723)  
563 [marine-120709-142723](https://doi.org/10.1146/annurev-marine-120709-142723), 2011.
- 564 Chen, J., Falk, M., Euskirchen, E., Paw U, K. T., Suchanek, T. H., Ustin, S. L., Bond, B. J.,  
565 Brosofske, K. D., Phillips, N., and Bi, R.: Biophysical controls of carbon flows in three  
566 successional Douglas-fir stands based on eddy-covariance measurements, *Tree Physiol.*, 22,  
567 169–177, <https://doi.org/10.1093/treephys/22.2-3.169>, 2002.
- 568 Chmura, G. L., Anisfeld, S. C., Cahoon, D. R., and Lynch, J. C.: Global carbon sequestration  
569 in tidal, saline wetland soils, *Glob. Biogeochem. Cycles*, 17,  
570 <https://doi.org/10.1029/2002GB001917>, 2003.
- 571 Clarke, P., J. and Jacoby, C. A.: Biomass and above-ground productivity of salt-marsh plants  
572 in South-eastern Australia, *Aust. J. Mar. Freshw. Res.*, 45, 1521–1528, 1994.
- 573 Duarte, C. M.: Reviews and syntheses: Hidden forests, the role of vegetated coastal habitats  
574 in the ocean carbon budget, *Biogeosciences*, 14, 301–310, [https://doi.org/10.5194/bg-14-301-](https://doi.org/10.5194/bg-14-301-575)  
575 [2017](https://doi.org/10.5194/bg-14-301-575), 2017.
- 576 Erickson, J. E., Peresta, G., Montovan, K. J., and Drake, B. G.: Direct and indirect effects of  
577 elevated atmospheric CO<sub>2</sub> on net ecosystem production in a Chesapeake Bay tidal wetland,  
578 *Glob. Change Biol.*, 19, 3368–3378, 2013.
- 579 Fagherazzi, S., Wiberg, P. L., Temmerman, S., Struyf, E., Zhao, Y., and Raymond, P. A.:  
580 Fluxes of water, sediments, and biogeochemical compounds in salt marshes, *Ecol. Process.*,  
581 2, 3, <https://doi.org/10.1186/2192-1709-2-3>, 2013.
- 582 Feagin, R. A., Forbrich, I., Huff, T. P., Barr, J. G., Ruiz-Plancarte, J., Fuentes, J. D., Najjar,  
583 R. G., Vargas, R., Vázquez-Lule, A., Windham-Myers, L., Kroeger, K. D., Ward, E. J.,  
584 Moore, G. W., Leclerc, M., Krauss, K. W., Stagg, C. L., Alber, M., Knox, S. H., Schäfer, K.  
585 V. R., Bianchi, T. S., Hutchings, J. A., Nahrawi, H., Noormets, A., Mitra, B., Jaimes, A.,  
586 Hinson, A. L., Bergamaschi, B., King, J. S., and Miao, G.: Tidal wetland gross primary  
587 production across the continental United States, 2000–2019, *Glob. Biogeochem. Cycles*, 34,  
588 e2019GB006349, <https://doi.org/10.1029/2019GB006349>, 2020.
- 589 Feher, L. C., Osland, M. J., Griffith, K. T., Grace, J. B., Howard, R. J., Stagg, C. L.,  
590 Enwright, N. M., Krauss, K. W., Gabler, C. A., Day, R. H., and Rogers, K.: Linear and  
591 nonlinear effects of temperature and precipitation on ecosystem properties in tidal saline  
592 wetlands, *Ecosphere*, 8, e01956, <https://doi.org/10.1002/ecs2.1956>, 2017.
- 593 Gedan, K. B., Silliman, B. R., and Bertness, M. D.: Centuries of human-driven change in salt  
594 marsh ecosystems, *Annu. Rev. Mar. Sci.*, 1, 117–141,  
595 <https://doi.org/10.1146/annurev.marine.010908.163930>, 2009.





- 596 Ghosh, S. and Mishra, D. R.: Analyzing the long-term phenological trends of salt marsh  
597 ecosystem across coastal Louisiana, *Remote Sens.*, 9, <https://doi.org/10.3390/rs9121340>,  
598 2017.
- 599 Giurgevich, J. R. and Dunn, E. L.: A comparative analysis of the CO<sub>2</sub> and water vapor  
600 responses of two *Spartina* species from Georgia coastal marshes, *Estuar. Coast. Shelf Sci.*,  
601 12, 561–568, [https://doi.org/10.1016/S0302-3524\(81\)80082-5](https://doi.org/10.1016/S0302-3524(81)80082-5), 1981.
- 602 Hilker, T., Hall, F. G., Coops, N. C., Lyapustin, A., Wang, Y., Nestic, Z., Grant, N., Black, T.  
603 A., Wulder, M. A., Kljun, N., Hopkinson, C., and Chasmer, L.: Remote sensing of  
604 photosynthetic light-use efficiency across two forested biomes: Spatial scaling, *Remote Sens.*  
605 *Environ.*, 114, 2863–2874, <https://doi.org/10.1016/j.rse.2010.07.004>, 2010.
- 606 Hill, A. C. and Vargas, R.: Methane and carbon dioxide fluxes in a temperate tidal salt marsh:  
607 comparisons between plot and ecosystem measurements, *J. Geophys. Res. Biogeosciences*,  
608 127, e2022JG006943, <https://doi.org/10.1029/2022JG006943>, 2022.
- 609 Howe, A. J., Rodríguez, J. F., Spencer, J., MacFarlane, G. R., and Saintilan, N.: Response of  
610 estuarine wetlands to reinstatement of tidal flows, *Mar. Freshw. Res.*, 61, 702–713, 2010.
- 611 Hughes, C. E., Kalma, J. D., Binning, P., Willgoose, G. R., and Vertzonis, M.: Estimating  
612 evapotranspiration for a temperate salt marsh, Newcastle, Australia, *Hydrol. Process.*, 15,  
613 957–975, <https://doi.org/10.1002/hyp.189>, 2001.
- 614 Huxham, M., Whitlock, D., Githaiga, M., and Dencer-Brown, A.: Carbon in the coastal  
615 seascape: how interactions between mangrove forests, seagrass meadows and tidal marshes  
616 influence carbon storage, *Curr. For. Rep.*, 4, 101–110, <https://doi.org/10.1007/s40725-018-0077-4>, 2018.
- 618 Kathilankal, J. C., Mozdzer, T. J., Fuentes, J. D., D’Odorico, P., McGlathery, K. J., and  
619 Ziemann, J. C.: Tidal influences on carbon assimilation by a salt marsh, *Environ. Res. Lett.*, 3,  
620 044010, <https://doi.org/10.1088/1748-9326/3/4/044010>, 2008.
- 621 Kljun, N., Calanca, P., Rotach, M. W., and Schmid, H. P.: A simple two-dimensional  
622 parameterisation for Flux Footprint Prediction (FFP), *Geosci Model Dev*, 8, 3695–3713,  
623 <https://doi.org/10.5194/gmd-8-3695-2015>, 2015.
- 624 Krauss, K. W., Lovelock, C. E., Chen, L., Berger, U., Ball, M. C., Reef, R., Peters, R.,  
625 Bowen, H., Vovides, A. G., Ward, E. J., and others: Mangroves provide blue carbon  
626 ecological value at a low freshwater cost, *Sci. Rep.*, 12, <https://doi.org/10.1038/s41598-022-12111-1>, 2022.
- 627 Lasslop, G., Reichstein, M., Papale, D., Richardson, A. D., Arneeth, A., BARR, A., STOY, P.,  
628 and WOHLFAHRT, G.: Separation of net ecosystem exchange into assimilation and  
629 respiration using a light response curve approach: critical issues and global evaluation, *Glob.*  
630 *Change Biol.*, 16, 187–208, <https://doi.org/10.1111/j.1365-2486.2009.02041.x>, 2010.
- 631 Lu, W., Xiao, J., Liu, F., Zhang, Y., Liu, C., and Lin, G.: Contrasting ecosystem CO<sub>2</sub> fluxes  
632 of inland and coastal wetlands: a meta-analysis of eddy covariance data, *Glob. Change Biol.*,  
633 23, 1180–1198, <https://doi.org/10.1111/gcb.13424>, 2017.
- 634 Mayen, J., Polsenaere, P., Lamaud, É., Arnaud, M., Kostyrka, P., Bonnefond, J.-M., Geairon,  
635 P., Gernigon, J., Chassagne, R., and Lacoue-Labarthe, T.: Atmospheric CO<sub>2</sub> exchanges



- 636 measured by eddy covariance over a temperate salt marsh and influence of environmental  
637 controlling factors, *Biogeosciences*, 21, 993–1016, 2024.
- 638 McLeod, E., Chmura, G. L., Bouillon, S., Salm, R., Björk, M., Duarte, C. M., Lovelock, C.  
639 E., Schlesinger, W. H., and Silliman, B. R.: A blueprint for blue carbon: toward an improved  
640 understanding of the role of vegetated coastal habitats in sequestering CO<sub>2</sub>, *Front. Ecol.*  
641 *Environ.*, 9, 552–560, <https://doi.org/10.1890/110004>, 2011.
- 642 Mcowen, C. J., Weatherdon, L. V., Bochove, J.-W. V., Sullivan, E., Blyth, S., Zockler, C.,  
643 Stanwell-Smith, D., Kingston, N., Martin, C. S., Spalding, M., and Fletcher, S.: A global map  
644 of saltmarshes, *Biodivers. Data J.*, 5, e11764, <https://doi.org/10.3897/BDJ.5.e11764>, 2017.
- 645 McVicar, T., Vleeshouwer, J., Van Niel, T., Guerschman, J., and Peña-Arancibia, J. L.:  
646 Actual Evapotranspiration for Australia using CMRSET algorithm. Version 1.0, 2022.
- 647 Mitsch, W. J. and Gosselink, J. G.: The value of wetlands: importance of scale and landscape  
648 setting, *Ecol. Econ.*, 35, 25–33, [https://doi.org/10.1016/S0921-8009\(00\)00165-8](https://doi.org/10.1016/S0921-8009(00)00165-8), 2000.
- 649 Moffett, K. B., Wolf, A., Berry, J. A., and Gorelick, S. M.: Salt marsh–atmosphere exchange  
650 of energy, water vapor, and carbon dioxide: Effects of tidal flooding and biophysical controls,  
651 *Water Resour. Res.*, 46, 2010.
- 652 Nahrawi, H., Leclerc, M. Y., Pennings, S., Zhang, G., Singh, N., and Pahari, R.: Impact of  
653 tidal inundation on the net ecosystem exchange in daytime conditions in a salt marsh, *Agric.*  
654 *For. Meteorol.*, 294, 108133, <https://doi.org/10.1016/j.agrformet.2020.108133>, 2020.
- 655 Navarro, A., Young, M., Macreadie, P. I., Nicholson, E., and Ierodiaconou, D.: Mangrove  
656 and saltmarsh distribution mapping and land cover change assessment for south-eastern  
657 Australia from 1991 to 2015, *Remote Sens.*, 13, <https://doi.org/10.3390/rs13081450>, 2021.
- 658 Otani, S. and Endo, T.: CO<sub>2</sub> flux in tidal flats and salt marshes, *Blue Carbon Shallow Coast.*  
659 *Ecosyst. Carbon Dyn. Policy Implement.*, 223–250, 2019.
- 660 Reents, S., Möller, I., Evans, B. R., Schoutens, K., Jensen, K., Paul, M., Bouma, T. J.,  
661 Temmerman, S., Lustig, J., Kudella, M., and Nolte, S.: Species-specific and seasonal  
662 differences in the resistance of salt-marsh vegetation to wave impact, *Front. Mar. Sci.*, 9,  
663 2022.
- 664 Schäfer, K. V. R., Duman, T., Tomasicchio, K., Tripathee, R., and Sturtevant, C.: Carbon  
665 dioxide fluxes of temperate urban wetlands with different restoration history, *Agric. For.*  
666 *Meteorol.*, 275, 223–232, <https://doi.org/10.1016/j.agrformet.2019.05.026>, 2019.
- 667 Seyfferth, A. L., Bothfeld, F., Vargas, R., Stuckey, J. W., Wang, J., Kearns, K., Michael, H.  
668 A., Guimond, J., Yu, X., and Sparks, D. L.: Spatial and temporal heterogeneity of  
669 geochemical controls on carbon cycling in a tidal salt marsh, *Geochim. Cosmochim. Acta*,  
670 282, 1–18, 2020.
- 671 Shepard, C. C., Crain, C. M., and Beck, M. W.: The protective role of coastal marshes: a  
672 systematic review and meta-analysis, *PLoS ONE*, 6, e27374,  
673 <https://doi.org/10.1371/journal.pone.0027374>, 2011.



- 674 Smith, J. A. M., Regan, K., Cooper, N. W., Johnson, L., Olson, E., Green, A., Tash, J., Evers,  
675 D. C., and Marra, P. P.: A green wave of saltmarsh productivity predicts the timing of the  
676 annual cycle in a long-distance migratory shorebird, *Sci. Rep.*, 10, 20658,  
677 <https://doi.org/10.1038/s41598-020-77784-7>, 2020.
- 678 Vázquez-Lule, A. and Vargas, R.: Biophysical drivers of net ecosystem and methane  
679 exchange across phenological phases in a tidal salt marsh, *Agric. For. Meteorol.*, 300,  
680 108309, <https://doi.org/10.1016/j.agrformet.2020.108309>, 2021.
- 681 Wang, Z. A., Kroeger, K. D., Ganju, N. K., Gonnecta, M. E., and Chu, S. N.: Intertidal salt  
682 marshes as an important source of inorganic carbon to the coastal ocean, *Limnol. Oceanogr.*,  
683 61, 1916–1931, <https://doi.org/10.1002/lno.10347>, 2016.
- 684 Ward, N. D., Megonigal, J. P., Bond-Lamberty, B., Bailey, V. L., Butman, D., Canuel, E. A.,  
685 Diefenderfer, H., Ganju, N. K., Goñi, M. A., and Graham, E. B.: Representing the function  
686 and sensitivity of coastal interfaces in Earth system models, *Nat. Commun.*, 11, 2458, 2020.
- 687 Wei, S., Han, G., Jia, X., Song, W., Chu, X., He, W., Xia, J., and Wu, H.: Tidal effects on  
688 ecosystem CO<sub>2</sub> exchange at multiple timescales in a salt marsh in the Yellow River Delta,  
689 *Estuar. Coast. Shelf Sci.*, 238, 106727, 2020.
- 690 Whitfield, A. K.: The role of seagrass meadows, mangrove forests, salt marshes and reed  
691 beds as nursery areas and food sources for fishes in estuaries, *Rev. Fish Biol. Fish.*, 27, 75–  
692 110, <https://doi.org/10.1007/s11160-016-9454-x>, 2017.
- 693 Xiao, J., Sun, G., Chen, J., Chen, H., Chen, S., Dong, G., Gao, S., Guo, H., Guo, J., Han, S.,  
694 Kato, T., Li, Y., Lin, G., Lu, W., Ma, M., McNulty, S., Shao, C., Wang, X., Xie, X., Zhang,  
695 X., Zhang, Z., Zhao, B., Zhou, G., and Zhou, J.: Carbon fluxes, evapotranspiration, and water  
696 use efficiency of terrestrial ecosystems in China, *Agric. For. Meteorol.*, 182–183, 76–90,  
697 <https://doi.org/10.1016/j.agrformet.2013.08.007>, 2013.
- 698